Paper IV

p53 protein biosignatures correlate with chemotherapy response and survival in acute leukemia

Nina Ånensen[1], Werner van Belle[3], Øystein Bruserud[1, 2], and Bjørn Tore Gjertsen[1,2]

[1]*Institute of Medicine, Hematology section, University of Bergen, Bergen, Norway*

[2]*Department of Internal Medicine, Hematology Section, Haukeland University Hospital, N-5021 Bergen, Norway.*

[3]*Norut IT, Postboks 6434, Forskningsparken, 9294 Tromsø*

Corresponding Author: Bjørn Tore Gjertsen,

Institute of Medicine, Hematology Section, Haukeland University Hospital,

University of Bergen, N-5021 Bergen, Norway.

Email: bjorn.gjertsen@med.uib.no

Phone: +4755975000

Fax: +4755972950

Key words: TP53, two-dimentional immunoblot, acute myeloid leukemia, in vivo

Running title: p53 protein as a bar code for cancer survival

Abstract

Multiple signaling networks target the anti-oncogene TP53 protein product by complex post-translational modulation, regulating stress responses like cell cycle arrest or cell death. The relation between wild type p53 protein and chemotherapy response is not fully understood. We have examined the relationship between the p53 protein profile of patient cancer cells and clinical data in samples from 39 acute myeloid leukemia and 8 acute lymphoblastic leukemia patients. The p53 profile was determined by two-dimensional gel electrophoresis immunoblot, recognizing the amino-terminal region that is modified by DNA damage activated kinases. Survival of patients correlated with strong expression of Δp53, while αp53 correlated with short survival. A similar but more significant correlation was found when remission response two weeks after chemotherapy was used as the clinical parameter. Conversely, the independent marker for disease relapse, Flt3 length mutation of the receptor tyrosine kinase Flt3, correlated with prominent αp53 isoforms. Inhibition of Flt3 by the kinase inhibitor PKC412 and down-regulation by small interfering RNA increased the pro-survival/pro-remission Δp53. These lines of evidence suggest that examinations of the p53 protein can decipher cell signaling network perturbations that direct clinical outcome in cancer, and that targeted signaling network therapy is reflected in the p53 profile.

Introduction

The anti-oncogene TP53 encodes the p53 protein, which mainly acts as a specific transcription factor that can halt progression through the cell cycle or initiate apoptosis upon activation by cell stress and genotoxic stimuli (Levine, 1997). In some malignancies, up to 70% of the cases may comprise mutations of TP53 (Levine et al., 1991), and specific mutations are proven to indicate chemoresistance (Geisler et al., 2003; Aas et al., 1996). Inactivation of the p53 protein can be achieved through up-regulation of proteins with inhibitory action towards wild type p53 (Haupt et al., 1997; Kubbutat et al., 1997), or through mutational hits in signaling pathways acting on p53 by post-translational modifications (Lonning, 2004; Staalesen et al., 2004). Post-translational modifications of the p53 protein are different in neoplastic cells compared to normal cells, and may be caused by environmental factors, mutations in signaling enzymes, mutations in adaptor molecules, or by epigenetic modulation of signaling pathways (Bernardi et al., 2004; Di Croce et al., 2002; Insinga et al., 2004). A manifold of post-translational combinations may be present on p53, with its 18 known phosphorylation sites in addition to several sites for acetylation (Gu and Roeder, 1997; Li et al., 2002; Lill et al., 1997), methylation (Chuikov et al., 2004), sumoylation (Rodriguez et al., 1999), ubiquitination (Li et al., 2002) and neddylation (Xirodimas et al., 2004). However, many of the phosphorylations are dispensable for the p53 function (Ashcroft et al., 1999; Thompson et al., 2004), and it is therefore important to investigate the interplay of multiple modifications in patient material to elucidate clinical significance.

Acute myeloid leukemia (AML) and acute lymphoblastic leukemia (ALL) are rapidly developing hematological cancers of the bone marrow where TP53 is rarely mutated, but where mutations in cell survival pathways are frequent and appearing in concert with altered transcription factors (Gilliland et al., 2004; Trecca et al., 1994). Prognosis of the AML patient is determined based on cytogenetic aberrations (Grimwade et al., 1998), disease free bone

marrow after first chemotherapy (Wheatley et al., 1999) and mutational status for the receptor tyrosine kinase Flt3 (Kottaridis et al., 2001). Mutation in the juxtamembranous region of Flt3 has been found to be a particularly strong and independent predictor of disease relapse after chemotherapy (Gale et al., 2005). We have recently suggested that signaling through phosphoprotein networks elucidate the underlying response mechanisms for chemotherapy, and may mirror the risk stratification in AML (Irish et al., 2004). A question that rose during this work was whether it was possible to decode this information at a complex junction in cancer cell chemosensitivity; at the post-translational modifications level of the p53 protein.

We visualized p53 protein isoform distribution in purified AML patient cells using two-dimensional gel electrophoresis and immunoblot (2DI). This method determined unique p53 biosignatures of 39 AML and 8 acute lymphoblastic leukemia (ALL) patient samples. After alignment and normalization of 2DIs we performed a correlation analysis with overall survival, response after first course of chemotherapy and Flt3 mutational status. We observed variations in p53 biosignature relating to these parameters. This suggested that adverse prognosis and relapse are associated with the expression of the αp53 isoform. Furthermore, the 2DI pattern correlating with Flt3-LM could be modified by inhibition of Flt3 by a small molecule inhibitor or small interfering RNA antagonizing Flt3 production. This indicates that the p53 biosignature responds to targeted therapeutics acting on signaling pathways contributing to chemoresistance.

Materials and Methods

Patients and separation of leukemia cells

The study was approved by the local Ethics Committee and samples collected after informed consent. During the period from 1992-2004 we collected peripheral blood blasts from 39 AML and 8 ALL patients. The clinical and biological characteristics of the patients are

presented in Table 1. Cell separation, cryostorage, culture and protein sample preparation of patient AML blasts were performed as previously described (Bruserud et al., 2003; Gjertsen et al., 2002; Irish et al., 2004).

Sample preparation

Cells for direct analysis of p53 were thawed carefully into StemSpan medium (Stem Cell Technologies, Vancouver, BC, Canada), washed in NaCl (9 mg/ml) and then lysed in 7% trichloroacetic acid. Protein precipitate was washed in 5% trichloroacetic and three times in water saturated ether to remove salts. Protein pellet was re-suspended in sample buffer for 2D gel electrophoresis (7 M urea, 2 M thiourea, 100 mM dithiotreitol, 1.5% Ampholyte 3-10, 0.5% Ampholyte 5-6, 0.5% 3-[(3-cholamidopropyl)dimethylammonio]-1-propanesulfonate). Molm-13 cell line (DSMZ, The German Resource Centre for Biological Material) was cultured in RPMI medium (Sigma Aldrich Inc.) with 10% fetal calf serum (HyClone, South Logan, UT, USA). Small molecule inhibitor PKC412 (Novartis, Switzerland) was used in 500 nM and added directly to the medium. Flt3 siRNA (Dharmacon Inc, Lafayette, Co, USA) was used in 300 nM and transfection was performed using the Amaxa system (AMAXA Biosystems, Germany) according to the manufacturers instructions. After treatment the cells were left to incubate for 24 hours at 37^{o}C before analysis using two-dimensional gel electrophoresis.

Two-Dimensional Gel Electrophoresis and immunoblotting

Two-dimensional gel electrophoresis (2D) was performed using 7 cm pH 3-10 (Zoom Strip, Invitrogen Corp., Carlsbad, CA, USA) isoelectric focusing gel strips, following the manufacturers' instructions. The focusing strips were incubated with Sample Rehydration Buffer (8 M urea, 1% 3-[(3-cholamidopropyl)dimethylammonio]-1-propanesulfonate, 20 mM dithiotreitol, 1.5% Ampholyte 3-10, 0.5% Ampholyte 5-6, Bromophenol Blue) over night at

room temperature to rehydrate the strips. Protein was added directly to the Rehydration buffer. Isoelectric focusing (IEF) was performed at 200 V for 40 minutes, 450 V for 30 minutes, 750 V for 30 minutes and 2000 V for 60 minutes. Following IEF, the strips were either stored at –80˚C until further use or equilibrated directly for 15 min in LDS sample buffer (Invitrogen Corp., Carlsbad, CA, USA) containing 100 mM dithiotreitol and then 15 min in LDS sample buffer containing 125 mM iodacetamide. For the second dimension the ZOOM strip was aligned in a 0.5% agarose solution added into the IEF well of a NuPAGE Novex 4 to 12 % Bis-Tris ZOOM Gel (Invitrogen Corp., Carlsbad, CA, USA). Electrophoresis was performed at 200 V for 60 minutes, after which the proteins were transferred to polyvinylidene fluoride membrane (Amersham Biosciences AB, Uppsala, Sweden) by standard electroblotting.

p53 protein was detected using primary Bp53-12 antibody (Santa Cruz Biotechnology, CA, USA) and secondary horse radish peroxidase conjugated mouse antibody (Jackson ImmunoResearch, West Grove, PA, USA) visualized using the Supersignal West Pico or Supersignal West Femto system (Pierce Biotechnology, Inc., Rockford, IL, USA). Chemiluminescence imaging was performed using a Kodak Image Station 2000R (Eastman Kodak Company, NY, USA).

Alignment and normalization of two-dimensional immunoblots

A critical task to properly correlate the p53 immunoblots with clinical data, is to correctly align all gels. The alignment was performed in three consecutive steps. First, a central common spot in the delta region was chosen in all blots with average location pixels (493,506). Then all blots were rotated to direct the delta-region spots horizontally. The rotation was performed using a cubic spline interpolation (Gonzalez and Woods, 1992) to avoid a typical “staircase” distortion of the image. The last step involved normalization of the Y-axis (molecular weight) by determining a scaling factor based on the vertical distance

between the alpha and delta regions (range on all blots is 29.7 pixels). This scaling factor was determined by the gel running time in the second dimension (separation based on molecular weight). After alignment the central common spot in the delta region had the average location pixels (300,150). There was no need to scale the pI axis, probably due to the combination of pre-made gel strips for isoelectric focusing and rigorous timing of the electrophoresis.

After alignment the gel expression levels were normalized within the [0:1] range. This removed all absolute protein expression information, thereby allowing us to study both the relative expression level within a gel as well as the morphology and pattern of different areas. Generation of a correlation image was performed for each clinical data set (survival, response after chemotherapy and Flt3 mutation status). Such an image consists of a test for every possible pixel position on the gel and depending on the outcome of the test, the pixel is colored differently. For every test two sets are generated. The first set is the relative expression level at that specific position. Given 89 gel images, we will have 89 different expression values; one for each gel. The second set contains a specified clinical feature associated with every gel, which again leads to 89 values. A correlation test is performed on those two vectors. When this correlation test is positive we use a green color, when the test is negative we use brown (Fig. 1).

The correlation used is rho-correlation (Spearman rank order correlation) (Press, 2002). This non-parametric correlation allows us to ignore the specific distributions in both the gel expression levels and the correlation test set. This means that we do not need to take into account the gray value distribution as produced by the camera. Equally, by using the Spearman correlation test, the impact of a non-uniform or unknown distribution is removed entirely, since the distribution in the result set may be unknown. The test itself correlates two datasets by replacing every element in the dataset with its specific rank in the dataset. Those

"normalized" datasets are then correlated using a standard linear Pearson correlation. To summarize; we define $E_{x,y,i}$ to be the ranked protein expression of gel i at apposition (x,y) and R_i the ranked result for gel i, then the correlation image is defined as

$$C_{x,y} = \frac{\sum_{i=0}^{n}(E_{x,y,i} - E_{x,y,\frac{n}{2}})(R_i - R_{\frac{n}{2}})}{\sqrt{\sum_{i=0}^{n}(E_{x,y,i} - E_{x,y,\frac{n}{2}})^2}\sqrt{\sum_{i=0}^{n}(R_i - R_{\frac{n}{2}})^2}}$$

Correlation does not necessarily imply a causal relationship. Depending on the number of elements and the presence of noise, we might detect correlations that occur by coincidence. To account for this possibility we used a significance test, typically associated with the Spearman correlation test. It is, in this context, defined as

$$S_{x,y} = 1 - C_{x,y}\sqrt{\frac{n-2}{1-C_{x,y}^2}}$$

If this number is close to 1 the probability of random data correlating with the given result set is low. Likewise, if this number is 0 the probability of the correlation being coincidence is high.

This significance measure is chosen arbitrarily, without understanding the noise fingerprint associated with the gels, as such it is merely an indicative guide. Specifically, there is very little known about the measurement errors, either in the gels or in the result set. As such, we cannot rely on the numerical value provided by the correlation measure. Instead, we may use the relative correlation indication in the image to understand the importance of a specific area. For instance, if a large area correlates negatively towards the result set, and within this area is something that correlates only slightly positively, then this located variance in correlation

suggests a spot region of importance. In this sense “no correlation” can be as important as detecting a strong correlation.

Algorithm for correlation analysis

The algorithm to correlate the images with clinical data was written in IDL v6.1 (Research Systems Inc., Boulder, CO). The algorithm takes input from a comma-separated file, passed as the first argument. The second argument denotes the data-containing column to correlate the gels with. The first cell of every row should contain the filename of the aligned and clipped image. Cells filled with '??' was removed before the correlation was performed, excluding patients who did not receive therapy from the analysis. All images need to have the same size. The two last arguments specify the width and height of the images.

```
PRO correlate_images, filename, column, VX, VY
lines = file2list(filename)

; Convert all the columns and rows to a 2 dimensional string
array
nroflines = n_elements(lines)
splitted = make_array(nroflines,50,/string)
for i = 0, nroflines - 1 do begin
params=strsplit(lines[i],':',/extract)
nrofparams=n_elements(params)
splitted[i,0:nrofparams-1]=params[*]
endfor

rc = reform(splitted[*,column])
indices = where(rc ne '??')
selected = splitted[indices,*]
```

```
nrselected = n_elements(indices)

result = make_array(nrselected,value=0.0)

; load all pictures in memory
all_pics = make_array(nrselected,VX,VY,value=0.0)
for i = 0, nrselected - 1 do begin
params = selected[i,*]
result[i]=params[column] + 0.0
file = params[0]
img = bytscl(tiff_input(file))
all_pics[i,*,*] = bytscl(img)
endfor

; Rho correlation
cor_pic = make_array(VX,VY,/double,value=0.0)
sig_pic = make_array(VX,VY,value=0.0)
for x = 0, VX - 1 do begin
for y = 0, VY - 1 do begin
r = r_correlate(reform(all_pics[*,x,y]),result)
cor_pic[x,y]=r[0]
sig_pic[x,y]=1.0-r[1]
endfor
endfor
show_correlation, cor_pic, sig_pic
end
```

Results

The biosignature of p53 protein was examined by two-dimensional immunoblotting (2DI) with antibody detection of the amino-terminal region. This part of p53 is targeted by several stress and chemoresistance related kinases. The pattern obtained with antibodies Bp53-12 equaled DO-1 and PAb1801/Ab-2, recognizing the p53 N-terminal epitope residues 20-25, 21-25 and 46-55, respectively (data not shown). The p53 profiles obtained varied between different cancer cell samples (Fig. 1). Each p53 2DI image was correlated to clinical parameters, as described in materials and methods and in Van Belle et al. 2005 (manuscript). We first wanted to examine if the p53 distribution provided any correlative information about therapy effect (Fig. 2A). Correlation of patient survival with p53 distribution showed a strong positive relationship (0.4) with the delta region and a negative relationship with the alpha region (Fig. 2A). To approach a validation of the survival correlation in AML, we tested the correlation of survival and p53 pattern in a separate set of ALL patients (Fig. 2B). The ALL correlation image suggests a similar result as obtained for AML: A strong positive correlation in the delta region (maximum correlation 0.49/-0.53). Unique features for the ALL survival analysis was one single negatively correlating delta spot and positive correlation in the alpha region, regions that reflect a lymphatic-myeloid lineage distinction between ALL and AML (Van Belle, manuscript).

One parameter used for risk stratification of chemoresistant patients is the presence of malignant cells after the first induction chemotherapy (Wheatley et al., 1999). Presence of ≤5% blasts in the bone marrow two weeks after start of chemotherapy was defined as remission. Clearly, the therapy remission/p53 correlation pattern (Fig. 3A) underscored the pro-survival patterns (Fig. 2). A strong positive correlation (0.59) of the delta spot was associated with remission after first course of chemotherapy and partly identical with the spots correlating with overall survival (0.46) (Fig. 2). The distribution of the distinct delta

spots appeared to be highly relevant for remission. A defined, horizontal distribution of spots was associated with remission while a more compact, vertically diffuse distribution was associated with patients resistant to first course chemotherapy (Fig. 3BC). Furthermore, a non-significant positive correlation with p63 was found in the remission analysis and with similar appearance as in the survival analysis (Fig. 2, 3).

Mutated receptor tyrosine kinases are a common feature of a wide range of malignancies, and in AML the frequent length mutation of receptor tyrosine kinase Flt3 is the single strongest marker for disease relapse (Gale et al., 2005). The test of correlation between p53 pattern and Flt3 length mutation (Flt3-LM) demonstrated the most positive correlation (0.26) for the alpha region of the p53 map (Fig. 4). This is consistent with the analysis of overall survival and p53, where the full-length region is negatively associated with long survival (Fig. 2A). The delta spot with positive correlation (0.2) with Flt3-LM was more basic than the corresponding region in the survival p53 map. This suggests that Flt3-LM alter p53 in line with patients with limited survival. Theoretically, inhibition of Flt3 should improve chemosensitivity and thereby survival in patients with AML. Based on our observation that the p53 patterns comprise information on relapse/chemosensitivity and survival, we examined if inhibition of Flt3 affected the p53 pattern. The AML derived cell line MOLM-13, a cell line that comprises Flt3-LM, was treated with the Flt3-targeting inhibitor PKC412 (500 nM) for 24 h (Fig. 5). PKC412 slightly increased the expression of Δp53 thereby bringing the p53 pattern closer to the survival and remission correlating patterns. PKC412 also induced a number of small molecular weight proteins resembling one survival correlating isoform found in ALL (Fig. 2B). These experiments were supported by transient transfection assays with small interfering RNA (300 nM, 24h) against Flt3 (Fig. 5).

Discussion

This study suggests that p53 protein patterns in acute leukemia indicate survival outcome after chemotherapy (Fig. 2). This is probable if the p53 patterns reflect post-translational modifications directed by the molecular perturbations behind the leukemogenesis, particularly since several of these mutations protect against chemotherapy-induced apoptosis. It is proposed that most acute leukemia are caused by a constitutively activated oncogenic tyrosine kinase combined with a perturbed transcription factor (Gilliland et al., 2004). Modified transcription factors in AML, e.g. PML-RAR, may affect p53 acetylation and thus influence on chemosensitivity (Insinga et al., 2004). Similarly, the most frequently mutated receptor tyrosine kinase in AML, Flt3, activates several signaling networks that phosphorylate p53 and decrease chemosensitivity *in vitro* (Jonsson et al., 2004; Komeno et al., 2005; Srinivasa and Doshi, 2002; Yeh et al., 2004).

Our mapping of p53 isoforms by 2DI has resulted in reproducible patterns with inter-patient variance. Non-stressed samples demonstrate limited or lacking reactivity with phosphospecific antibodies (Irish, Ånensen et al, manuscript). The charge distribution seen in the alpha and delta forms may be caused by phosphorylated residues without corresponding phospho-specific antibodies, but may also be limited by the antibody detection limits. Acetyl-p53 specific immunodetection has so far not resolved the p53 distribution. The difference in size between alpha and delta may be caused by splice variants although we know that the 47 kDa Δp53 isoform does not correspond to the previously reported p47 (Courtois et al., 2002), as both the Bp53-12 and Ab-2 antibodies produce the same protein pattern (data not shown). p47 would not be detected by Bp53-12 as this isoform lacks the epitope for this antibody. The size difference between the two main isoforms is ~6 kDa, and thereby too small to be caused by ubiquitination, sumoylation or neddylation. The p53 protein has at least 18 residues that may be phosphorylated in addition to 7 known lysine residues targeted by acetylation,

methylation, ubiquitination, sumoylation and neddylation. Some of these residues may be critical, but based on previous reports the redundancy of modifications may be extensive in such an important protein. This may implicate that a 2DI profile would be a highly informative way of examining complex parameters like chemoresistance.

Poor survival after chemotherapy in AML is predominantly the result of disease relapse. An important factor in disease relapse is the cancer cell's threshold for undergoing apoptosis during chemotherapy. Defined phosphorylations of p53 are related to cell death and block in cell proliferation (Mayo et al., 2005; Taylor and Stark, 2001). It may therefore be the balance between different p53 isoforms that sets the threshold for response to chemotherapy. The reason for stronger p53 delta region correlation in the remission analysis compared with the survival analysis could be explained by the nature of these clinical parameters (Figs. 2, 3). Overall survival is a long-term parameter, affected by tumor-host interactions, serious infections and eventually by other diseases than the malignancy, factors relatively unrelated to the leukemia cell death induction by chemotherapy. In contrast, remission after first chemotherapy is the result of tumor debulkment within the short time span of two weeks, and is directly affected by the cancer cell chemosensitivity.

Mutated receptor tyrosine kinases are a common feature of a wide range of malignancies, and targeted therapies are in some cases established in the clinic (Baselga and Arteaga, 2005; Heinrich et al., 2002). The strongest independent marker for disease relapse in AML is length mutation (LM) in the juxtamembrane domain of the receptor tyrosine kinase Flt3 of the AML cells (Gale et al., 2005). This mutation is related to chemoresistance mediated by the constitutively activated Flt3 kinase (Levis and Small, 2003). Signaling from the activated Flt3 kinase may affect p53 function. The kinases p38 and ERK1/2 have distinct phosphorylation sites on p53 (Komeno et al., 2005; Yeh et al., 2004), kinases that in some leukemia cell lines

are activated by Flt3 (Komeno et al., 2005; Srinivasa and Doshi, 2002). Furthermore, Flt3 may activate PKB/AKT (Jonsson et al., 2004), a kinase that may alter the apoptotic regulation of p53 (Lin et al., 2002). Recently, activation analysis of these phosphoprotein signaling networks has been suggested to predict chemoresistance in cancer when compared to clinical markers like Flt3 mutation and remission (Irish et al., 2004). This indirectly supports our observation that these signaling pathways may modulate the p53 pattern *in vivo.*

We have presented several lines of evidence of a correlation between certain p53 patterns and chemosensitivity (Figs. 2-4), and that these p53 patterns may be altered by pathway targeted therapy (Fig. 5). Further studies are needed to validate this observation and to determine the nature of the p53 modifications that may be involved in specific protein regulation. Due to p53's central localization in signaling networks we hypothesize that the p53 patterns contain signaling information of relevance for therapy. The system of p53 modulation indicated in this study may be caused by phenocopying, allowing us to categorize the multitude of mutations in oncogenic kinases and transcription factors by classes of p53 patterns. Reading the p53 protein biosignature may therefore be an effective alternative to mapping of mutations or epigenetic perturbations in signaling pathways and thus be a fruitful guide to customize future signaling targeted therapy.

Acknowledgements

This study was supported by The Research Council of Norway's National Program for Research in Functional Genomics (FUGE, grant no. 151859), and the Norwegian Cancer Society (Kreftforeningen).

Table 1. Clinical and biological characteristics of acute myeloid leukemia patients

Patient #	Sex	Age	FAB	Cytogenetic Abnormality	Flt3-Abnormality	Resistance 1. course	Survival (Months)
1	M	30	M3	t(15;17)	LM	+	0
2	M	29	M4/5	Normal	LM	+	12
3	M	29	M4/5	Normal	LM	+	12
4	F	56	M5a	T(9;11)	WT	-	9
5	M	82	M1	47XY,+19(8)/46,XY(7)	WT	nd	8
6	M	71	M4	47XY,+11	LM	nd	0
7	M	69	M2	inv(16)	WT	-	26
8	F	64	M1	46XX,del(11)(q14)/46XX,del(11)(q14),del(20)(q11)/ 50XX,del(11)(q14),+21,+21,+21,+21	WT	+	3
9	M	86	M2	Normal	WT	nd	2
10	F	45	M4	Normal	WT	-	15
11	M	33	M5	Normal	LM	-	9
12	M	39	M3	t(15;17)	LM	-	19
13	F	34	M5a	t(9;11)	KD	-	24
14	M	60	M4/5	Normal	LM	-	23
15	F	75	M5	Normal	LM	+	5
16	M	74	M5	nd	LM	nd	1
17	F	59	M2	-7	WT	+	3
18	F	79	M5	46XX,del(12)(p11)/46XX,del(12)(p11),add(11)(p15)	KD	nd	1
19	F	36	M5	t(9;11)	WT	-	52
20	F	58	M1	Normal	WT	+	5
21	M	82	M5	45X	WT	nd	0
22	M	72	M5	Normal	WT	+	5
23	F	77	M2	42-46XX-5,del(5?)	WT	+	9
24	M	74	M0/1	90-94,XXYY	WT	nd	2
25	F	78	M4/5	47-49,XX,-4,-5,+der(8)	WT	nd	0
26	F	44	M1	del7q22	LM	+	1
27	M	64	M4/5	Normal	LM	+	0
28	F	51	M2	Normal	LM	-	10
29	F	64	M1	43,XX,-7	WT	nd	0
30	M	56	M2	Normal	LM	+	2
31	M	69	M1/2	nd	WT	nd	2
32	F	61	M4/5	Normal	WT	+	2
33	M	33	M1	+4	LM	+	31
34	F	58	M2	Normal	LM	+	6
35	M	79	M1	Normal	LM	nd	0
36	F	63	M4	Normal	LM	+	6
37	M	65	M2	46XY,t(13;15)(q10;q10),-17,+21,+22	WT	nd	0
38	M	36	M2	46,XY,der(9)(ins22q12;q34)	WT	+	3
39	M	43	M2	Normal	WT	nd	0
40	F	23	ALL	t(9;22)		-	24
41	M	84	ALL	nd		nd	0
42	M	60	ALL	44XY,del 7q,11q,-18,-21		+	9
43	F	54	ALL	t(9;22		+	11
44	M	27	ALL	t(4;11)		-	52
45	M	79	ALL	nd		nd	3
46	M	22	ALL	45XYdic(7;9)(q11;q11)		-	42
47	F	29	ALL	t(9;22)		-	51

Figure legends

Figure 1. Analysis of p53 in two-dimensional immunoblot and correlation with clinical data. AML patients show great heterogeneity in p53 isoform profile and several forms of the protein are detected. The main forms are denominated alpha (presumably full length p53) and delta (presumably truncated variant). Cell lysates from primary AML cells were processed for two-dimensional gel electrophoresis and immunoblot as described in Materials and methods. After digital acquisition, the images were aligned and normalized before the correlation analysis. Clinical data (blue line) and the relative protein expression (red line) in each image were tested for correlation using a non-parametric correlation analysis. This generated a correlation image, where positive correlation is colored green and negative correlation is colored brown. A masked correlation picture was made to test causal relationship by the Spearman correlation test (not shown). See Material and methods for details on gel processing, image analysis and correlation tests.

Figure 2. p53 protein patterns in acute leukemia at time of diagnosis and its correlation with survival after chemotherapy. The p53 protein pattern of treated patients (n=39; Table I) were correlated to months of survival after start of treatment (A; left, correlation; right, significance of correlation). The profiles of correlation and significance for the alpha and delta regions are shown in inserts. Increasing intensity of green color indicates long survival, while increasing intensity of brown color indicates short survival. A similar analysis was performed for treated ALL patients (n=8) (B).

Fig. 3. Remission response to induction chemotherapy and its correlation with the p53 protein pattern. Success or failure to achieve complete hematological remission after first chemotherapy was analyzed related to p53 patterns (A, left, correlation; right, significance of correlation). The profiles of correlation and significance for the alpha and delta regions are

shown in inserts. Increasing intensity of green color indicates successful response to chemotherapy, while increasing intensity of brown color indicates therapy failure. A digitized picture based on the mean protein signal indicated that the distribution and shape of the delta isoform was the main characteristic associated with remission. Patients that went into remission had a defined, horizontal resolution between delta spots, while p53delta in patients that did not enter remission had a more compact, vertically diffuse shape (B). Patients representing therapy responders and non-responders demonstrated similar distributions as the mean images (C).

Figure 4. Receptor tyrosine kinase Flt3 mutational status in relation to p53 protein pattern. Status for mutation in the juxtamembrane region of Flt3 was determined at diagnosis, and presence or absence of Flt3 length mutation (LM) was correlated with p53 patterns (A, left, correlation; right, significance of correlation). The profiles of correlation and significance for the alpha and delta regions are shown in inserts. Increasing intensity of green color indicates presence of Flt3-LM, while increasing intensity of brown color indicates wild type gene for Flt3.

Figure 5. Modulation of p53 protein patterns by targeting of Flt3. The receptor tyrosine kinase Flt3 was inhibited by the small molecule inhibitor PKC412 (500 nM, 24h) and Flt3 siRNA (300 nM, 24h). Inhibition of Flt3 increased the acidity of αp53 and slightly increased the expression of Δp53. Flt3 inhibition also led to the expression of smaller molecular weight protein isoforms. Non-relevant siRNA had no impact on p53 protein patterns (data not shown).

References

Ashcroft, M., Kubbutat, M. H., and Vousden, K. H. (1999). Regulation of p53 function and stability by phosphorylation. Mol Cell Biol *19*, 1751-1758.

Baselga, J., and Arteaga, C. L. (2005). Critical update and emerging trends in epidermal growth factor receptor targeting in cancer. J Clin Oncol *23*, 2445-2459.

Bernardi, R., Scaglioni, P. P., Bergmann, S., Horn, H. F., Vousden, K. H., and Pandolfi, P. P. (2004). PML regulates p53 stability by sequestering Mdm2 to the nucleolus. Nat Cell Biol *6*, 665-672.

Bruserud, O., Hovland, R., Wergeland, L., Huang, T. S., and Gjertsen, B. T. (2003). Flt3-mediated signaling in human acute myelogenous leukemia (AML) blasts: a functional characterization of Flt3-ligand effects in AML cell populations with and without genetic Flt3 abnormalities. Haematologica *88*, 416-428.

Chuikov, S., Kurash, J. K., Wilson, J. R., Xiao, B., Justin, N., Ivanov, G. S., McKinney, K., Tempst, P., Prives, C., Gamblin, S. J.*, et al.* (2004). Regulation of p53 activity through lysine methylation. Nature *432*, 353-360.

Courtois, S., Verhaegh, G., North, S., Luciani, M. G., Lassus, P., Hibner, U., Oren, M., and Hainaut, P. (2002). DeltaN-p53, a natural isoform of p53 lacking the first transactivation domain, counteracts growth suppression by wild-type p53. Oncogene *21*, 6722-6728.

Di Croce, L., Raker, V. A., Corsaro, M., Fazi, F., Fanelli, M., Faretta, M., Fuks, F., Lo Coco, F., Kouzarides, T., Nervi, C.*, et al.* (2002). Methyltransferase recruitment and DNA hypermethylation of target promoters by an oncogenic transcription factor. Science *295*, 1079-1082.

Gale, R. E., Hills, R., Kottaridis, P. D., Srirangan, S., Wheatley, K., Burnett, A. K., and Linch, D. C. (2005). No evidence that FLT3 status should be considered as an indicator for transplantation in acute myeloid leukemia (AML): an analysis of 1135 patients excluding acute promyelocytic leukemia from the UK MRC AML10 and 12 trials. Blood.

Geisler, S., Borresen-Dale, A. L., Johnsen, H., Aas, T., Geisler, J., Akslen, L. A., Anker, G., and Lonning, P. E. (2003). TP53 gene mutations predict the response to neoadjuvant treatment with 5-fluorouracil and mitomycin in locally advanced breast cancer. Clin Cancer Res *9*, 5582-5588.

Gilliland, D. G., Jordan, C. T., and Felix, C. A. (2004). The molecular basis of leukemia. Hematology (Am Soc Hematol Educ Program), 80-97.

Gjertsen, B. T., Oyan, A. M., Marzolf, B., Hovland, R., Gausdal, G., Doskeland, S. O., Dimitrov, K., Golden, A., Kalland, K. H., Hood, L., and Bruserud, O. (2002). Analysis of acute myelogenous leukemia: preparation of samples for genomic and proteomic analyses. J Hematother Stem Cell Res *11*, 469-481.

Gonzalez, R. C., and Woods, R. E. (1992). Digital image processing (Reading, Mass., Addison-Wesley).

Grimwade, D., Walker, H., Oliver, F., Wheatley, K., Harrison, C., Harrison, G., Rees, J., Hann, I., Stevens, R., Burnett, A., and Goldstone, A. (1998). The importance of diagnostic

cytogenetics on outcome in AML: analysis of 1,612 patients entered into the MRC AML 10 trial. The Medical Research Council Adult and Children's Leukaemia Working Parties. Blood *92*, 2322-2333.

Gu, W., and Roeder, R. G. (1997). Activation of p53 sequence-specific DNA binding by acetylation of the p53 C-terminal domain. Cell *90*, 595-606.

Haupt, Y., Maya, R., Kazaz, A., and Oren, M. (1997). Mdm2 promotes the rapid degradation of p53. Nature *387*, 296-299.

Heinrich, M. C., Blanke, C. D., Druker, B. J., and Corless, C. L. (2002). Inhibition of KIT tyrosine kinase activity: a novel molecular approach to the treatment of KIT-positive malignancies. J Clin Oncol *20*, 1692-1703.

Insinga, A., Monestiroli, S., Ronzoni, S., Carbone, R., Pearson, M., Pruneri, G., Viale, G., Appella, E., Pelicci, P., and Minucci, S. (2004). Impairment of p53 acetylation, stability and function by an oncogenic transcription factor. Embo J *23*, 1144-1154.

Irish, J. M., Hovland, R., Krutzik, P. O., Perez, O. D., Bruserud, O., Gjertsen, B. T., and Nolan, G. P. (2004). Single cell profiling of potentiated phospho-protein networks in cancer cells. Cell *118*, 217-228.

Jonsson, M., Engstrom, M., and Jonsson, J. I. (2004). FLT3 ligand regulates apoptosis through AKT-dependent inactivation of transcription factor FoxO3. Biochem Biophys Res Commun *318*, 899-903.

Komeno, Y., Kurokawa, M., Imai, Y., Takeshita, M., Matsumura, T., Kubo, K., Yoshino, T., Nishiyama, U., Kuwaki, T., Osawa, T.*, et al.* (2005). Identification of Ki23819, a highly potent inhibitor of kinase activity of mutant FLT3 receptor tyrosine kinase. Leukemia *19*, 930-935.

Kottaridis, P. D., Gale, R. E., Frew, M. E., Harrison, G., Langabeer, S. E., Belton, A. A., Walker, H., Wheatley, K., Bowen, D. T., Burnett, A. K.*, et al.* (2001). The presence of a FLT3 internal tandem duplication in patients with acute myeloid leukemia (AML) adds important prognostic information to cytogenetic risk group and response to the first cycle of chemotherapy: analysis of 854 patients from the United Kingdom Medical Research Council AML 10 and 12 trials. Blood *98*, 1752-1759.

Kubbutat, M. H., Jones, S. N., and Vousden, K. H. (1997). Regulation of p53 stability by Mdm2. Nature *387*, 299-303.

Levine, A. J. (1997). p53, the cellular gatekeeper for growth and division. Cell *88*, 323-331.

Levine, A. J., Momand, J., and Finlay, C. A. (1991). The p53 tumour suppressor gene. Nature *351*, 453-456.

Levis, M., and Small, D. (2003). FLT3: ITDoes matter in leukemia. Leukemia *17*, 1738-1752.

Li, M., Luo, J., Brooks, C. L., and Gu, W. (2002). Acetylation of p53 inhibits its ubiquitination by Mdm2. J Biol Chem *277*, 50607-50611.

Lill, N. L., Grossman, S. R., Ginsberg, D., DeCaprio, J., and Livingston, D. M. (1997). Binding and modulation of p53 by p300/CBP coactivators. Nature *387*, 823-827.

Lin, Y., Brown, L., Hedley, D. W., Barber, D. L., and Benchimol, S. (2002). The death-promoting activity of p53 can be inhibited by distinct signaling pathways. Blood *100*, 3990-4000.

Lonning, P. E. (2004). Genes causing inherited cancer as beacons to identify the mechanisms of chemoresistance. Trends Mol Med *10*, 113-118.

Mayo, L. D., Rok Seo, Y., Jackson, M. W., Smith, M. L., Rivera Guzman, J. R., Korgaonkar, C. K., and Donner, D. B. (2005). Phosphorylation of human p53 at serine 46 determines promoter selection and whether apoptosis is attenuated or amplified. J Biol Chem.

Press, W. H. (2002). Numerical recipes in C++ : the art of scientific computing, 2nd edn (Cambridge, Cambridge University Press).

Rodriguez, M. S., Desterro, J. M., Lain, S., Midgley, C. A., Lane, D. P., and Hay, R. T. (1999). SUMO-1 modification activates the transcriptional response of p53. Embo J *18*, 6455-6461.

Srinivasa, S. P., and Doshi, P. D. (2002). Extracellular signal-regulated kinase and p38 mitogen-activated protein kinase pathways cooperate in mediating cytokine-induced proliferation of a leukemic cell line. Leukemia *16*, 244-253.

Staalesen, V., Falck, J., Geisler, S., Bartkova, J., Borresen-Dale, A. L., Lukas, J., Lillehaug, J. R., Bartek, J., and Lonning, P. E. (2004). Alternative splicing and mutation status of CHEK2 in stage III breast cancer. Oncogene *23*, 8535-8544.

Taylor, W. R., and Stark, G. R. (2001). Regulation of the G2/M transition by p53. Oncogene *20*, 1803-1815.

Thompson, T., Tovar, C., Yang, H., Carvajal, D., Vu, B. T., Xu, Q., Wahl, G. M., Heimbrook, D. C., and Vassilev, L. T. (2004). Phosphorylation of p53 on key serines is dispensable for transcriptional activation and apoptosis. J Biol Chem *279*, 53015-53022.

Trecca, D., Longo, L., Biondi, A., Cro, L., Calori, R., Grignani, F., Maiolo, A. T., Pelicci, P. G., and Neri, A. (1994). Analysis of p53 gene mutations in acute myeloid leukemia. Am J Hematol *46*, 304-309.

Wheatley, K., Burnett, A. K., Goldstone, A. H., Gray, R. G., Hann, I. M., Harrison, C. J., Rees, J. K., Stevens, R. F., and Walker, H. (1999). A simple, robust, validated and highly predictive index for the determination of risk-directed therapy in acute myeloid leukaemia derived from the MRC AML 10 trial. United Kingdom Medical Research Council's Adult and Childhood Leukaemia Working Parties. Br J Haematol *107*, 69-79.

Xirodimas, D. P., Saville, M. K., Bourdon, J. C., Hay, R. T., and Lane, D. P. (2004). Mdm2-mediated NEDD8 conjugation of p53 inhibits its transcriptional activity. Cell *118*, 83-97.

Yeh, P. Y., Chuang, S. E., Yeh, K. H., Song, Y. C., Chang, L. L., and Cheng, A. L. (2004). Phosphorylation of p53 on Thr55 by ERK2 is necessary for doxorubicin-induced p53 activation and cell death. Oncogene *23*, 3580-3588.

Aas, T., Borresen, A. L., Geisler, S., Smith-Sorensen, B., Johnsen, H., Varhaug, J. E., Akslen, L. A., and Lonning, P. E. (1996). Specific P53 mutations are associated with de novo resistance to doxorubicin in breast cancer patients. Nat Med *2*, 811-814.

Supplemental data: 3D models of survival correlations

APPENDIX

```
FUNCTION FILE2LIST, fn
  nlines = FILE_LINES(fn)
  sarr = STRARR(nlines)
  OPENR, unit, fn, /GET_LUN
  READF, unit, sarr
  FREE_LUN, unit
  return, sarr
end

PRO show_correlation_grey, cp, t_pic, m_pic
  mean_pic = sqrt(sqrt(m_pic))
  cor_pic = cp
  print, 'Maximum significance', max(t_pic)
  print, 'Minimum significance', min(t_pic)
  print, 'Maximum positive correlation', max(cor_pic)
  print, 'Maximum negative correlation', min(cor_pic)
  DDD = size(cp,/dim)
  VX = ddd[0]
  VY = ddd[1]

  ; green = 0 200 50
  ; brown = 200 100 0

  ; the normal one
  cor_pic=127.0+float(cor_pic)*127.0/max(abs(cor_pic))

  ; only the significant correlation
  wcor_pic = double(cp) * double(t_pic)
  wcor_pic=127.0+float(wcor_pic)*127.0/max(abs(wcor_pic))

  cor_pic[0,0]=0
  wcor_pic[0,0]=0
  cor_pic[1,0]=255
  wcor_pic[1,0]=255
  window, 2, title='Correlation', ret=2, xsize=vx, ysize=vy
  tvscl, cor_pic

  ; significance
  window, 1, title='Significance', ret=2, xsize=vx, ysize=vy
  tvscl, wcor_pic

end
```

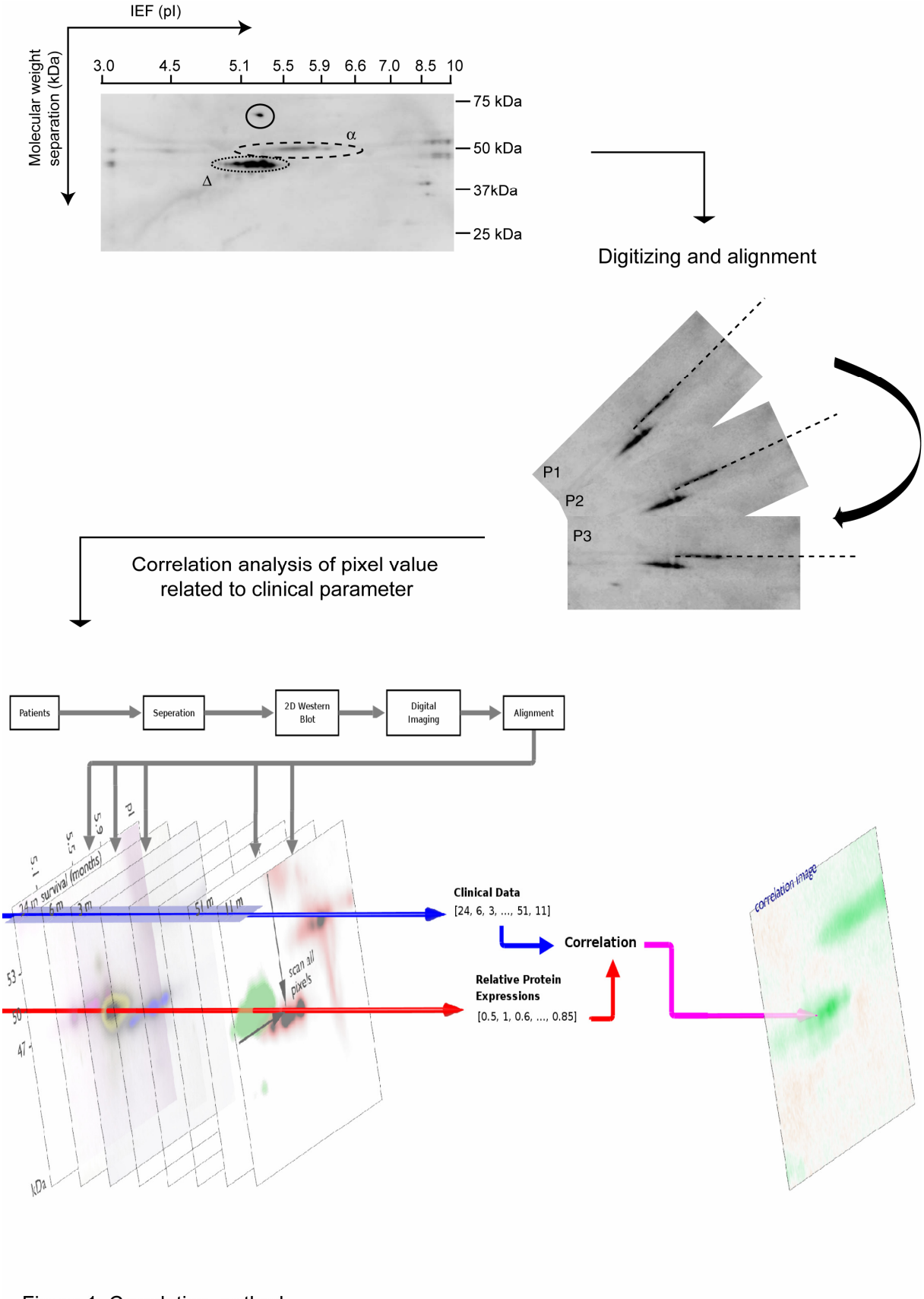

Figure 1. Correlation method

A

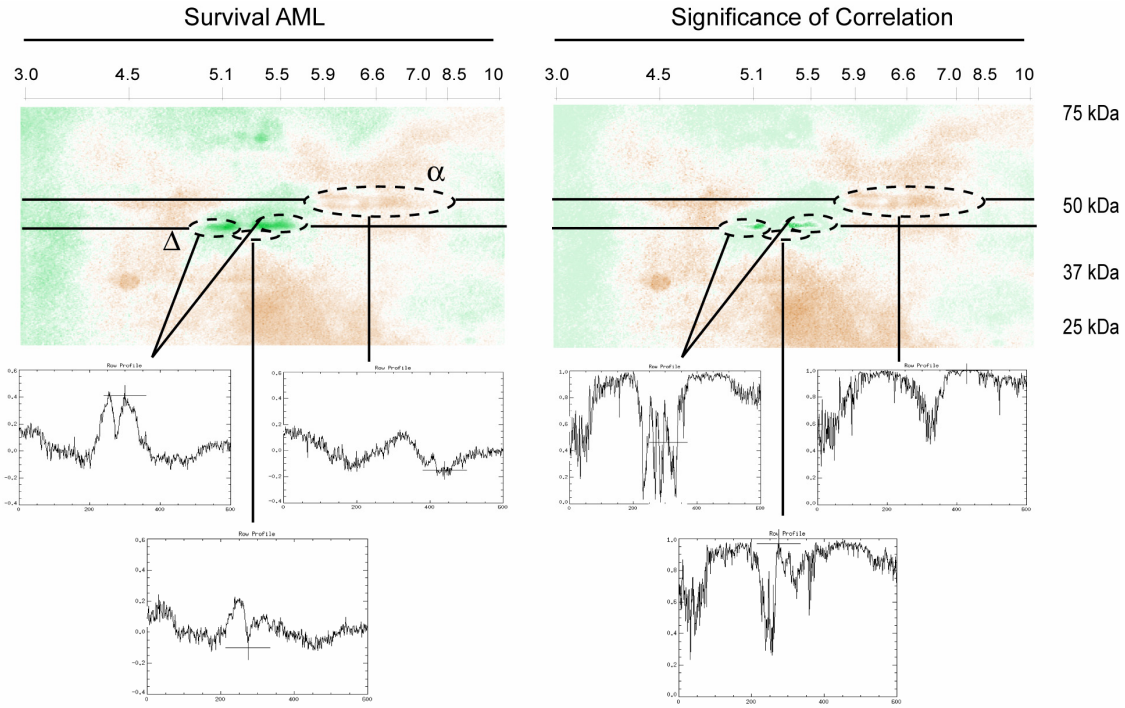

Maximum correlation: 0.459
Maximum anti-correlation: -0.304

B

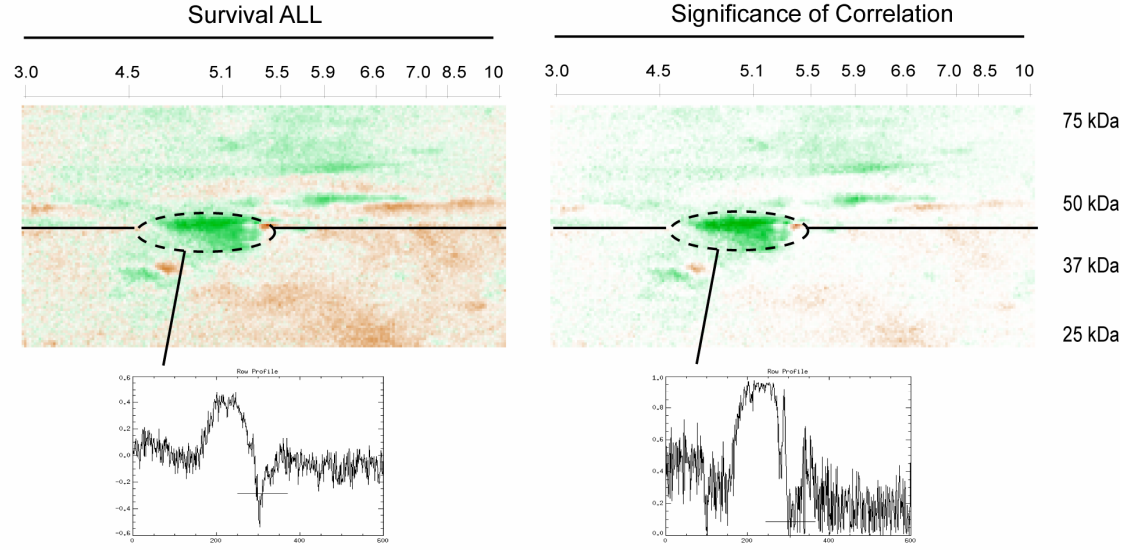

Maximum correlation: 0.495
Maximum anti-correlation: -0.536

Figure 2. Survival

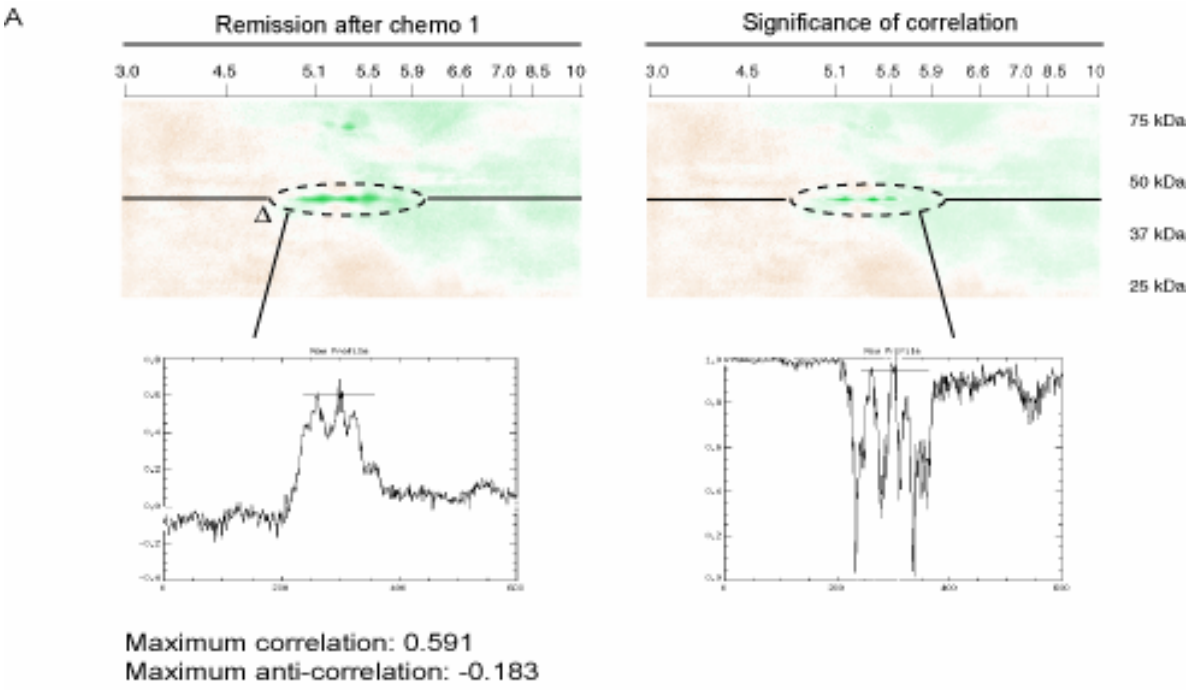

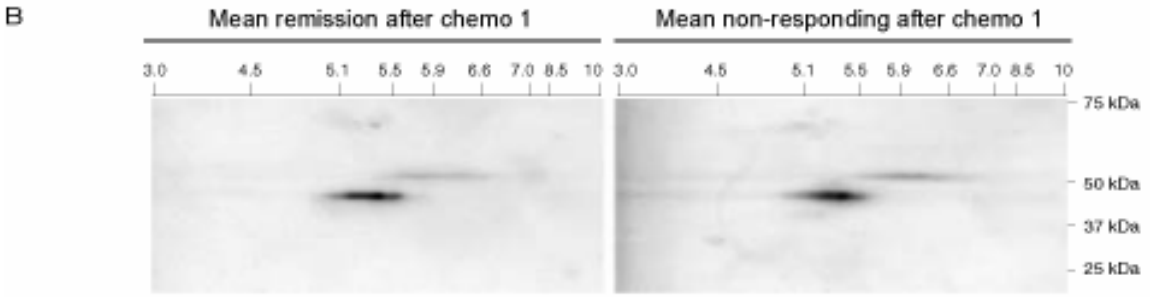

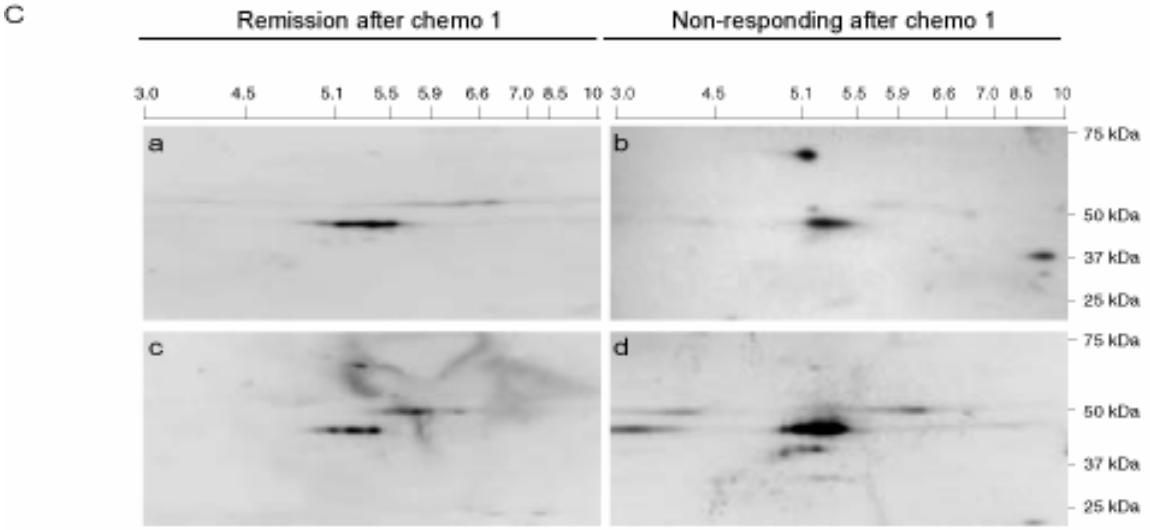

Figure 3. Remission

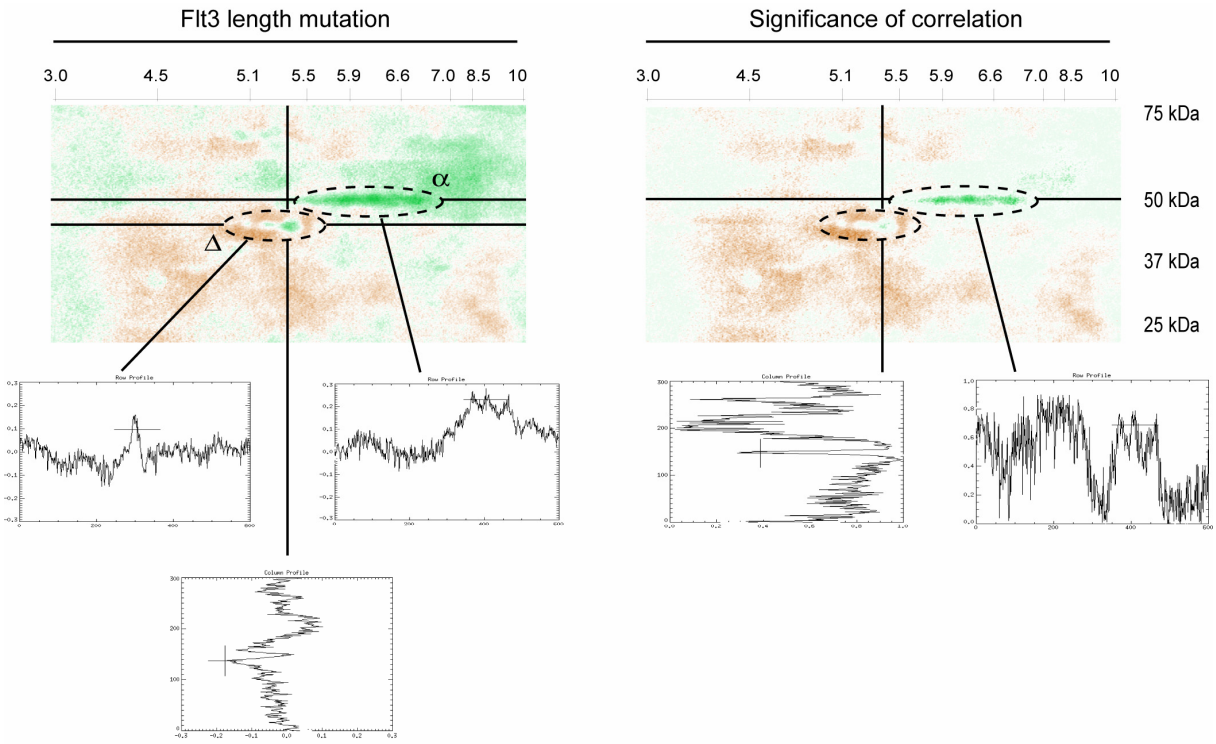

Maximum correlation: 0.264
Maximum anti-correlation: -0.149

Figure 4. Flt3 length mutation

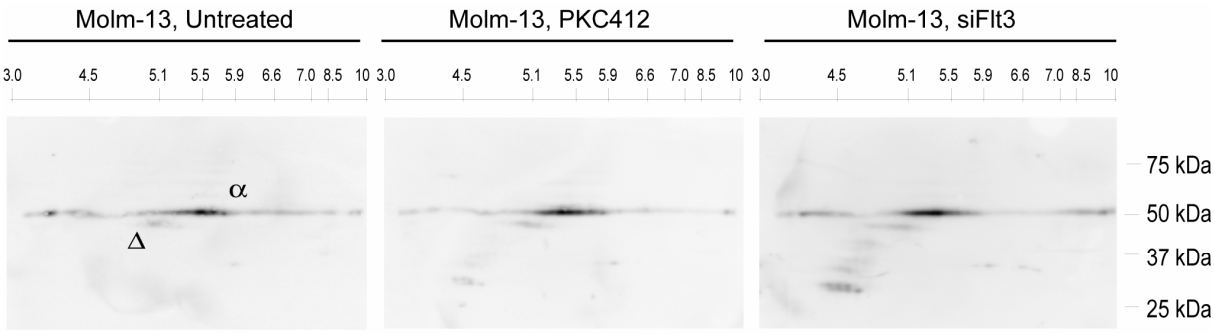

Figure 5. Flt3 inhibition